FULL PAPER

Dalton
www.rsc.org/dalton

Metallation effects on the thermal interconversion of atropisomers of di(orthomethylarene)-substituted porphyrins

Paul G. Plieger,[a] Anthony K. Burrell,*[a] Geoffrey B. Jameson[b] and David L. Officer[b]

[a] *Actinide, Catalysis and Separations Chemistry, C-SIC, Los Alamos National Laboratories, MS J514, Los Alamos, NM 87545, USA. E-mail: burrell@lanl.gov*

[b] *Institute of Fundamental Sciences, Massey University, Private Bag 11222, Palmerston North, New Zealand*

Received 15th October 2003, Accepted 20th November 2003
First published as an Advance Article on the web 12th December 2003

A new series of *meso*-substituted diaryl free-base and metalloporphyrins have been prepared. Each arene has been substituted with both a methyl group in the *ortho* position and a formyl group in the *meta* position. Rotation of the arene units is prevented at room temperature due to the steric restrictions imposed by the flanking methyl groups at the porphyrin β-pyrrolic positions on the methyl groups at the *ortho* position on the *meso*-substituted arene unit. This allowed the αα and αβ atropisomers of this porphyrin to be separated and characterised. X-Ray crystallographic determination of the structure of the free-base porphyrin revealed a very flat porphyrin core. Metallation resulted in the isolation and characterisation of the nickel, zinc and copper derivatives. The assignments of the αα and αβ isomers are confirmed by X-ray crystallographic determination of the structures of the Cu(II) analogues. The copper αα structure exhibits a very twisted porphyrin core, the copper αβ structure is also distorted, but to a lesser degree. The activation energy for rotation has been calculated for each of the 2H, Ni and Zn derivatives. The energy required to rotate the arene ring increases in the order Ni < Zn ~ 2H. No significant difference in the free energy of rotation was observed between experiments carried out with the αα and αβ isomers.

Introduction

Atropisomerism arises when steric hindrance caused by adjacent atoms prevents an otherwise unhindered single bond from rotating. Atropisomerism is important in porphyrin chemistry, as the room temperature isomers (usually *ortho*-substituted tetraarenes) are locked in place, which allows a degree of geometric control to be exerted on the porphyrin substituents. In the mid 1970's, Collman and co-workers utilised the α_4 atropisomer of *ortho*-substituted *meso*-tetraphenylporphyrin as a structural scaffold to create picket-fence porphyrins, which acted as biological mimics for dioxygen-binding hemoproteins.[1] More recently, others have utilised porphyrin atropisomers in applications as diverse as catalysis and molecular recognition,[2] as well as continuing to explore their uses as mimics for biological systems.[3,4] The ability to control substituents orthogonal to the porphyrin plane has also been exploited in the area of supramolecular chemistry.[5]

Atropisomerism in porphyrins with *meso*-aryl substituents was first described by Gottwald and Ullman.[6] Since this first account, atropisomerism has been seen in tetra-,[3,7–11] di-[12–15] and mono-substituted porphyrin[16] systems containing *meso*-aryl and -alkyl substituents,[16] both with hydrogen and larger flanking β-pyrrolic substituents. For porphyrins that are *meso*-arene substituted, atropisomerism usually arises due to *ortho* substitution on the arene ring. However, in at least a few cases, suitably bulky substituents have led to atropisomerism of *meta*-arene substituted porphyrins.[17]

A handful of studies have been undertaken to identify the factors contributing to the ease of arene rotation in porphyrin atropisomers. In the first comprehensive study of atropisomerism of tetraaryl-substituted porphyrins, Freitag and Whitten examined both thermally induced and photoinduced atropisomerism of a series of picket-fence porphyrins and demonstrated that a correlation exists between non-polar core distortions and the atropisomerisation rates.[7] For example, introduction of a metal ion into the porphyrin core resulted in a rigid porphyrin backbone, as seen by an increase in the relative energy required for atropisomer interconversion. These results have been mirrored in other systems.[10,13,16] Gust *et al*. found that it was easier to rotate the phenyl rings of the dicationic form of the *ortho*-methoxy substituted arene porphyrin than those of the corresponding free base, as determined by the average free energy of rotation.[8] A similar effect was found by Zimmer *et al.* for their tetra-catechol substituted porphyrin.[11] A theoretical study of aryl ring rotation in arylporphyrins has been conducted by Okuno and co-workers.[18] They examined the atropisomerism of a mono-arene substituted porphyrin and concluded that a considerable deformation of the porphyrin ring in the transition-state region was required for aryl ring rotation.[18]

Almost all these studies of porpyrin atropisomerism have concentrated on tetraaryl-substituted porphyrins. The simpler diaryl systems have been largely overlooked.[12] The removal of two adjacent aryl rings from the *meso* positions changes the rigidity of the porphyrin core and this is likely to reduce the energy required to deform the porphyrin core and, hence, rotate the substituted arene ring. To date, little information has been reported on the energies associated with isomer interconversion of the 5,15-di-*meso* substituted arene analogues.[13,15,19]

We have recently synthesised a new di-*meso* substituted arylporphyrin building block for use in the synthesis of larger porphyrin arrays. This has provided us with an opportunity to investigate the atropisomerism of this class of porphyrin.

Results and discussion

Porphyrin synthesis

The diaryl-substituted porphyrins were constructed *via* a five-step synthetic strategy, starting from 4-methylbenzaldehyde (Scheme 1). By using dichloromethane as the reaction medium instead of the reported 1,2-dichloroethane,[20] a substantial increase in the yield of **1** was obtained (89 *vs*. 63%). Protection of benzaldehyde **1** to give **2** was achieved quantitatively using 2,2-dimethyl-1,3-propanediol in the presence of *p*-toluenesulfonic acid (*p*-TsOH). Substitution of **2** using ^{t}BuLi and DMF at −78 °C and subsequent hydrolysis produced **3** as a light yellow peach-scented oil. This was purified *via* column chromatography before the porphyrin condensation

DOI: 10.1039/b312898a

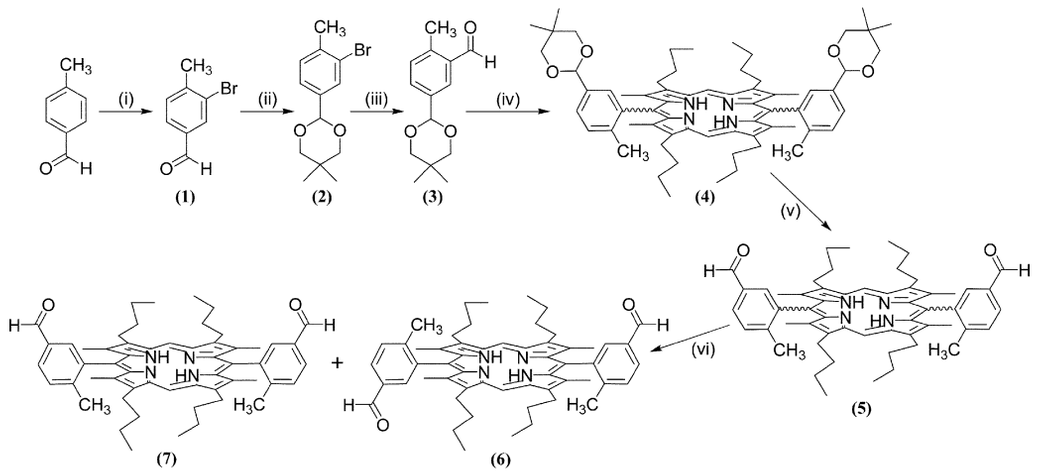

Scheme 1 *Reagents and conditions*: (i) $AlCl_3$, CH_2Cl_2, Br_2, argon; (ii) $HOCH_2C(CH_3)_2CH_2OH$, *p*-TsOH, C_6H_6, reflux, 18 h; (iii) ^{t}BuLi, THF, −78 °C, DMF, argon, HCl(aq); (iv) 3,3′-di-n-butyl-4,4′-dimethyl-2,2′-dipyrrolylmethane, CH_2Cl_2, TFA, DBU, *p*-chloranil; (v) $CHCl_3$–TFA–H_2O, rt, 1 h, argon; (vi) chromatography.

was attempted. The diaryl-substituted porphyrin **4** was formed *via* an acid-catalysed condensation, using trifluoroacetic acid (TFA). Initial attempts to separate the resulting atropisomers failed, as the difference in polarity was insufficient to allow clean separation. However, once the diacetal groups were deprotected, the differences in the polarity of porphyrins **6**-H_2 and **7**-H_2 was sufficient as to allow careful separation *via* chromatography. The overall yield for a multi-gram synthesis of the isomeric mixture of porphyrins was 32%.

Separation and identification of the atropisomers

The diphenylporphyrins with *ortho*-methyl substituents exist as atropisomeric mixtures, due to the restricted rotation of the phenyl rings. Careful column chromatography on silica gel (1 : 1 CH_2Cl_2–hexane doped with 0–0.5% diethyl ether) resulted in the isolation of the αβ isomer, **6**-H_2, followed by the αα isomer, **7**-H_2 (1 : 1 CH_2Cl_2–hexane doped with 1% diethyl ether). The relative stereochemistry of the two free-base isomers was initially assigned on the basis of polarity, with the less polar αβ isomer eluting first. The assignment was further confirmed by examining the ^{1}H NMR signal corresponding to the protons on the α-carbon of the n-butyl groups in the 2, 8, 12 and 18 positions of the porphyrin skeleton. For the symmetrically equivalent αα isomer, it is expected the chemical shifts of the signals corresponding to the protons on the α-carbon will be equivalent, resulting in the observation of a simple 8H triplet. This was indeed observed in the ^{1}H NMR of the more polar isomer. The signals corresponding to the α-carbon protons in the αβ isomer were more complex, with the observation of two closely overlapping triplets due the diastereotopic nature of the CH_2 groups.

Solid-state structures

Conclusive assignment of the geometries was completed by single crystal X-ray examination of the porphyrins and their metallated derivatives. The molecular structure of **6**-H_2 is shown in Fig. 1, with structural parameters listed in Table 1. The asymmetric unit contains half of the molecule, which lies across a crystallographic inversion centre. This crystallographic symmetry imposes an αβ symmetry on the molecule, which allows us to assign this porphyrin as the αβ atropisomer. However, the presence of disorder in the structure with the methyl groups and the aldehydes (50 : 50 occupation factors), makes unequivocal assignment of the atropisomer impossible.

The 24 atoms of the porphyrin macrocycle all lie within 0.05 Å of their least-squares plane. The aryl groups are slightly tilted away from the porphyrin core by angles of 173.30 and 176.95° (for molecules I and II, respectively). The plane of

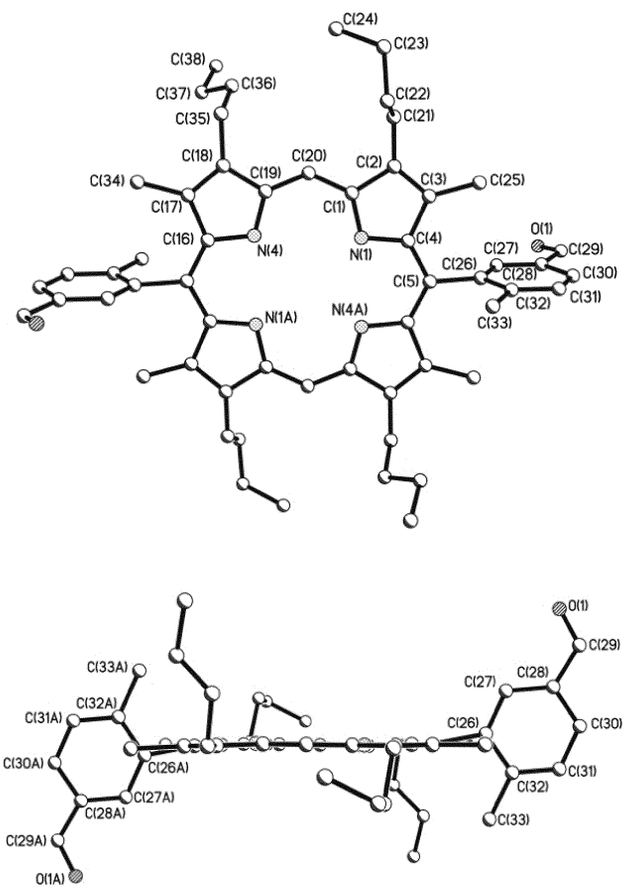

Fig. 1 Solid-state structure of **6**-H_2. The formyl group in the *meta*-aryl position is 50% disordered over both sites (for clarity, only one is shown). The H atoms and n-butyl disorder have been removed for clarity. Atoms labelled with an A are related by symmetry (1/2 − *x*, 3/2 − *y*, −*z*) to those with the same number.

each aryl ring is almost perpendicular [86.0(4) and 89.3(4)° for molecules I and II, respectively] with respect to the plane of the porphyrin.

Preparation of both copper complexes enabled the conclusive assignment of the relative atropisomers. Crystals of **6**-Cu and **7**-Cu suitable for X-ray diffraction were grown by the slow evaporation of concentrated $CHCl_3$–MeOH solutions containing the appropriate atropisomer. Diffuse solvent equivalent to three chloroform molecules (343 e per cell) per unit cell was treated in the manner described by van der Sluis and Spek [21] for **7**-Cu. The molecular structure of **6**-Cu is shown in Fig. 2, with structural parameters listed in Table 1. Both of these structures

Table 1 X-Ray parameters for the porphyrins **6**-H_2, **6**-Cu and **7**-Cu

	6-H_2	**6**-Cu	**7**-Cu
Empirical formula	$C_{28}H_{33}N_2O$ [a]	$C_{56}H_{64}N_4O_2Cu$	$C_{56}H_{64}N_4O_2Cu$
Formula wt.	827.11	888.65	888.65
T/K	150	150	150
Crystal system	Monoclinic	Monoclinic	Triclinic
Space group	$C2/c$	$P2(1)/c$	$P\bar{1}$
a/Å	32.2970(7)	27.2070(6)	17.8253(5)
b/Å	11.8287(3)	10.8242(2)	18.6667(5)
c/Å	13.4306(3)	15.8465(3)	31.1012(7)
α/°	90	90	85.070(1)
β/°	111.321(1)	93.121(1)	77.896(1)
γ/°	90	90	89.020(1)
Z	8	4	8
U/Å^3	4779.7(2)	4659.8(2)	10081.1(5)
Reflections observed	4201	9777	85186
Independent reflections	2781	6955	35333
R_{int}	0.0454	0.0447	0.0767
R_1	0.0938	0.0493	0.0866
wR_2	0.2685	0.1334	0.2598

[a] The molecular formula for **6**-H_2 is $C_{56}H_{66}N_4O_2$.

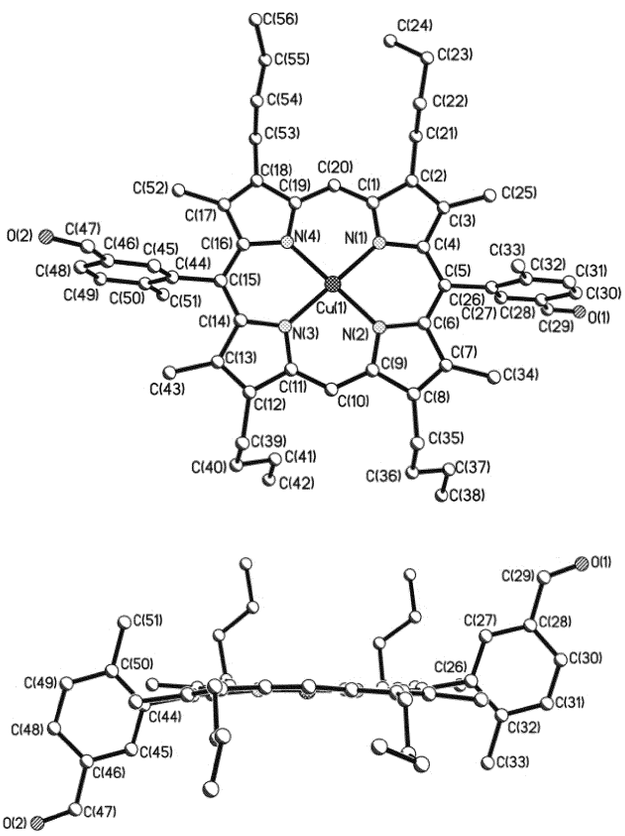

Fig. 2 Solid-state structure of **6**-Cu, The H atoms and n-butyl disorder have been removed for clarity.

enable conclusive assignment of the atropisomers, which matches our predictions from the NMR data and the relative polarity of the atropisomers.

The 24 atoms of the porphyrin macrocycle in **6**-Cu are more ruffled compared to **6**-H_2, with deviations of up to 0.15 Å (*cf.* 0.05 Å for the free base) from their least-squares plane and the Cu^{2+} atom sitting essentially within this plane (0.01 Å). The aryl groups are tilted above and below on either side from the porphyrin core by angles of 172.2 and 170.5°, more obtuse than for the free-base equivalent. The slight distortion in the porphyrin core is further evidenced in the β-pyrrolic methylene groups, which are further above and below the porphyrin plane (−0.14 to +0.28 Å) than in **6**-H_2. The planes of each aryl ring are again almost perpendicular [86.0(2) and 85.2(2)°] with respect to the plane of the porphyrin. There are four independent molecules of **7**-Cu in the asymmetric unit, three of which are considerably more distorted/ruffled than **6**-Cu (Fig. 3). The porphyrin core atoms of molecules A, C and D correlate reasonably well with one another (Fig. 4), (<0.17 correlation error for the 24 core porphyrin atoms), the porphyrin core atoms of B have poor correlations with the other three molecules (>0.40), but correlate reasonably with the porphyrin core atoms of **6**-Cu (~0.19). The 24 core atoms of the three molecules A, C and D protrude by as much as 0.468 Å from their least-squares plane. However, the Cu^{2+} atoms associated with these molecules still sit within this plane (−0.044–0.065 Å). Each arene ring is less tilted above and below the porphyrin core as compared with **6**-Cu (average angle of 174.8°). The distortion in the porphyrin core is further evidenced by the large

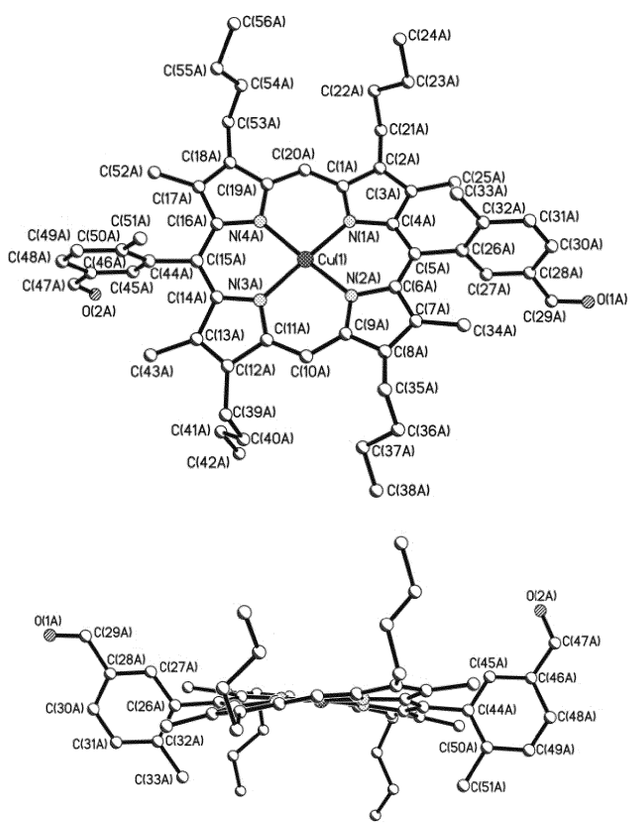

Fig. 3 Solid-state structure of one of four independent molecules of **7**-Cu in the asymmetric unit. The H atoms have been removed for clarity.

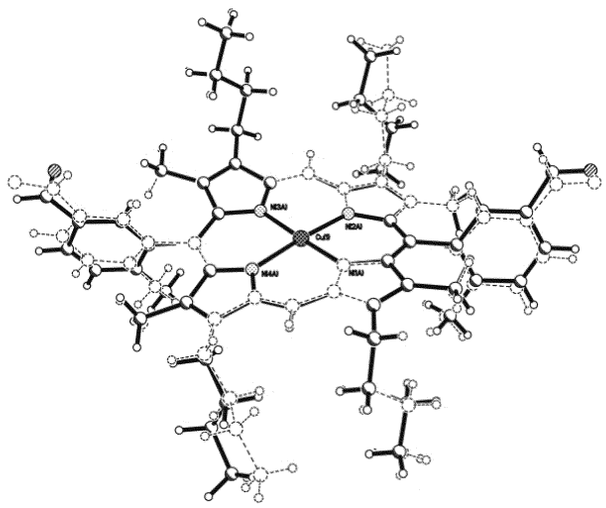

Fig. 4 An overlay of two of the four independent porphyrins of **7**-Cu (A and C) showing the close correlation between the 24 core atoms of each porphyrin.

displacements from the 24-atom porphyrin plane of the methylene groups attached at the β-pyrrolic positions of the porphyrin (average displacement 0.55 Å, maximum displacement 0.92 Å). The angles between the planes between the aryl groups and the porphyrin cores are now less acute, resulting in further twisting of the arene rings away from perpendicular [typical angles range from 75.1(6) and 87.5(6)°] with respect to the plane of the porphyrin. The overall visual effect for these three porphyrins (A, C and D) is that it appears that the porphyrin core has been twisted along the C5–C15 axis (Fig. 3). The core atoms of the fourth independent molecule in the asymmetric unit (B) sit flatter than those of the other three molecules, resulting in a less twisted appearance, more akin to the core atoms of **6**-Cu (Fig. 2). The planes of the aryl groups are closer to perpendicular [81.6(4) and 88.3(5)°] with respect to the plane of the porphyrin. The methylene groups attached to the porphyrin β-pyrrolic positions are less out of plane (0.42 Å) than their more twisted counterparts, yet, surprisingly, the arene rings are further above and below the porphyrin core plane then in molecules A, C and D.

Kinetic studies of the isomerisation

Atropisomerism was expected in these porphyrins due to the steric hindrance imposed by the presence of *ortho*-methyl substituents on the aryl rings. Rates of atropisomerisation were determined for **6**-H_2, **6**-Zn and **6**-Ni in toluene. The rate of atropisomerisation for **7**-Ni was also determined. The rate constants at various temperatures and the activation parameters for the atropisomerisation of **6**-X (where X = H_2, Ni and Zn) to a mixture of **6**-X and **7**-X are shown in Table 2, and are compared with those of selected literature examples in Table 3. These results indicate that the nickel complexes have lower activation barriers to rotation than both the free-base and zinc porphyrins. The free energy of activation for rotation of the phenyl ring increases in the following order: **7**-Ni ≈ **6**-Ni < **6**-Zn ≈ **6**-H_2. A similar trend has been observed for *ortho*-substituted tetraphenylporphyrins.[7] The $\Delta G^{\ddagger}$ values for **6**-Ni and **7**-Ni lie within experimental error, despite a three-fold difference in their atropisomerisation rates. The free energy of activation for rotation of the phenyl ring of the free-base porphyrin **6**-H_2 is similar in magnitude to those for the related *ortho*-phenylene substituted (picket fence) tetraphenylporphyrins of Freitag and Whitten,[7] yet is larger than the energies for the diarylporphyrins of Young and Chang.[15] The rates of interconversion of the studied diarylporphyrins are also slower than those observed by Young and Chang[15] and by Redman and Sanders.[13] The picket fence tetraarylporphyrins have protons on the flanking pyrroles,

Table 2 Activation parameters and atropisomerisation rates of the porphyrins studied. Equation used as obtained from Laidler and Meiser;[22] parameters have their usual meanings[a]

	T/K	K/s^{-1}	$\Delta G^{\ddagger}$[b]/kJ mol^{-1}
6-H_2	409	3.5171×10^{-5}	136
	401	1.1816×10^{-5}	137
	394	6.9339×10^{-6}	136
	386	2.6557×10^{-6}	137
	379	1.1917×10^{-6}	137
	Average $\Delta G^{\ddagger}$ = 137 kJ mol^{-1}		
	$\Delta H^{\ddagger}$[c] = 137 kJ mol^{-1}		
	$\Delta S^{\ddagger}$[d] = 2 J mol^{-1} K^{-1}		
6-Zn	409	5.6637×10^{-6}	142
	401	3.0588×10^{-6}	142
	394	2.1933×10^{-6}	140
	386	7.9347×10^{-7}	141
	379	4.5804×10^{-7}	142
	Average $\Delta G^{\ddagger}$ = 141 kJ mol^{-1}		
	$\Delta H^{\ddagger}$[c] = 105 kJ mol^{-1}		
	$\Delta S^{\ddagger}$[d] = −90 J mol^{-1} K^{-1}		
6-Ni	409	4.4629×10^{-4}	128
	394	1.0257×10^{-4}	127
	379	3.2982×10^{-5}	126
	365	8.2428×10^{-6}	125
	352	2.0204×10^{-7}	125
	Average $\Delta G^{\ddagger}$ = 126 kJ mol^{-1}		
	$\Delta H^{\ddagger}$[c] = 108 kJ mol^{-1}		
	$\Delta S^{\ddagger}$[d] = −49 J mol^{-1} K^{-1}		
7-Ni	394	3.55213×10^{-4}	122
	379	1.17929×10^{-4}	122
	365	2.63703×10^{-5}	123
	Average $\Delta G^{\ddagger}$ = 122 kJ mol^{-1}		
	$\Delta H^{\ddagger}$[c] = 105 kJ mol^{-1}		
	$\Delta S^{\ddagger}$[d] = −45 J mol^{-1} K^{-1}		

[a] Uncertainty in measurement for compounds under study ±2.5%. [b] Calculated from $\Delta G^{\ddagger} = RT[\ln k - \ln(\kappa T/\hbar)]$. [c] Calculated from an Arrenhius plot. [d] Calculated from $\Delta S^{\ddagger} = R[\ln A - 1 - \ln(\kappa T/\hbar)]$.

whereas our system has methyl substituents. It has also been postulated that diarylporphyrin skeletons are more flexible than their tetraaryl analogues.[15] It appears that in our work, both factors effectively cancel each other out. The reasons for the substantial increase in the free energy of activation for rotation of **6**-H_2 as compared to the porphyrins of Young and Chang are currently unclear. All of these porphyrins are diaryl with flanking β-pyrrolic methyl substituents, yet the difference in ΔG between the two systems is ~20%. The relative sizes of the *ortho* substituents will contribute to some of this difference, as will inductive interactions caused by the addition of the *meta*-substituted formyl group (in the present examples). It has been shown that the addition of *para* substituents affects the free energy of activation for rotation in free-base and metallated tetraarylporphyrins by as much as 9.6 kJ mol^{-1}.[8,23] A similar effect may also be present for *meta*-substituted arylporphyrins.

The **6**-Zn porphyrin has a free energy of activation for rotation similar in magnitude to that of **6**-H_2, but significantly larger than for the **6**-Ni or **7**-Ni porphyrins. Previous authors[7] have attributed this to the porphyrin core becoming rigid upon coordination of zinc, which locks the porphyrin core into a flat configuration, thus increasing the energy barrier to rotation. Zinc porphyrins also have a propensity to acquire a fifth ligand in an axial position, whether it be solvent or other coordination ligands. It is possible that this ligation has a significant effect on the flexibility of the porphyrin core. This effect has been seen with other axially ligated metalloporphyrins.[23] In our examples, there is no external ligand, nor is there any evidence of coordinated solvent in their ^{1}H NMR spectra. Potentially, the porphyrin complex could also dimerise, but again, no evidence

Table 3 Comparison of atropisomerisation rates and activation parameters of the porphyrins studied herein with those of literature examples

Porphyrin	β-Pyrrolic substituent	Arene *o*-substituent	*T*/K	k(386 K)/s^{-1}	$\Delta H^{\ddagger}$/ kJ mol^{-1}	$\Delta S^{\ddagger}$/ J mol^{-1} K^{-1}	$\Delta G^{\ddagger}$(386 K)/ kJ mol^{-1}	Ref.
5,15-Diarylporphines								
6-H_2	CH_3	CH_3	379–409	2.66×10^{-6}	137	2.0	137	This study
6-Zn	CH_3	CH_3	379–409	8.79×10^{-7}	105	−89.6	140	This study
6-Ni	CH_3	CH_3	351–409	5.92×10^{-5}	108	−48.8	127	This study
7-Ni	CH_3	CH_3	365–394	1.96×10^{-4}	104	−45.4	123	This study
DPE[a]	CH_3	NH_2	360–396	1.1×10^{-2} [b]	~113 [c]	~8 [c]	109 [b]	15
cis-(Acetamide)$_2$DPE[d]	CH_3	4-^{t}Bu-*N*-benzamide	388–414	9.74×10^{-4} [e]	~134 [e]	~41 [c]	118 [e]	15
5,10,15,20-Tetraphenyl-21*H*,23*H*-porphines								
Pivalylamide	H	Pivalyl-*N*-amide	369–406	3.1×10^{-5} [c]	112	−41.8	128 [c]	7
Hexadecylamide	H	Hexadecan-*N*-amide	352–406	3.3×10^{-4} [d]	115	−16.7	122 [d]	7
Propylamide	H	Propyl-*N*-amide	349–408	2.4×10^{-4} [a]	115	−16.7	122 [a]	7
Propylamide-H_4	H	Propyl-*N*-amide					110 [e]	7
Propylamide-Ni	H	Propyl-*N*-amide					108 [e]	7
Propylamide-Zn	H	Propyl-*N*-amide					131 [e]	7

[a] DPE = 2,2′-(2,8,12,18-tetraethyl-3,7,13,17-tetramethyl-21*H*,23*H*-porphine-5,15-diyl)bisbenzenamine. [b] At 385 K. [c] Calculated from ref. 15. [d] (4-*tert*-Butyl)-*N*-benzamide replaces amine at *ortho* position of aryl. [e] At 388 K. [f] At 384 K. [g] At 387 K. [h] At 383 K.

(an upfield shift in the CHO NMR signal, for example) was observed in our spectra. Both of these factors may contribute to the observed differences in the rate of atropisomerism in zinc porphyrins in other systems. A more plausible explanation of the difference in the entropy of activation between the nickel and zinc derivatives lies in the much smaller ionic radius of Ni(II), which leads to strongly ruffled porphyrin conformations in order to shorten the Ni–N(porphyrin) separation. Zn(II), on the other hand, forces the central hole of a completely planar porphyrin dianion to expand slightly (from 2.015 to 2.035 Å), leaving a rather more flexible porphyrin. Relative to Zn(II) porphyrins, the Ni(II) analogue has lower entropy (more ordered) and, hence, a *smaller*, less unfavourable entropy change to the highly ordered transition state. For the nickel and zinc derivatives, the enthalpy of activation is very similar, leading to the marked difference observed in the free energy of activation between them. The free-base porphyrin, on the other hand (see Table 2), has a noticeably higher enthalpy of activation coupled with a negligible entropy of activation. This is consistent with an activated complex in which the internal pyrrolic N–H ⋯ N hydrogen bonds are weakened through distortion of the porphyrin (contribution to $\Delta H^{\ddagger}$), which acquires additional flexibility (whence $\Delta S^{\ddagger} \approx 0$). A relatively small $\Delta S^{\ddagger}$ is also seen for free-base tetraaryl-substituted porphyrins with non-bulky *ortho* substituents.[7] Further work is underway to elaborate the factors that influence the rate of atropisomerism in metalloporphyrins.

Conclusions

A new series of *meso*-substituted diaryl free-base and metalloporphyrins have been prepared. Each arene has been substituted with both a methyl group in the *ortho* position and a formyl group in the adjacent *meta* position. Rotation of the arene units is prevented at room temperature by the steric restrictions imposed by the presence of flanking methyl groups at the β-pyrrolic positions on the methyl groups. This allowed the αα and αβ atropisomers of this porphyrin to be separated and characterised. X-Ray crystallographic determination of the free-base porphyrin reveals a very flat porphyrin core. Metallation of **6**-H_2 provided nickel, zinc and copper derivatives. The assignments of αα and αβ atropisomers were confirmed by the X-ray crystallographic determination of the Cu(II) analogues. The copper αα structure exhibits a very twisted porphyrin skeleton; the copper αβ structure is similar but less distorted. The entropic and enthalpic contributions to the free energy of rotation of the arene rings have been determined for each of the H_2, Ni(II) and Zn(II) derivatives. The free energy of activation for rotation of the arene ring increased in the order Ni < Zn ≈ H_2. The origin of the differences between the Ni and Zn derivatives most likely lies in the entropy of activation; for the free base, a significantly higher enthalpy of activation and much less negative entropy of activation was observed compared to the metallated derivatives. Further work is needed to assess the contributing factors. A three-fold difference in atropisomerisation rates between the Ni(II) αα and αβ isomers did not lead to a significant difference in their free energy of rotation.

Experimental

Materials and methods

Melting points were recorded on a Kofler hot stage and are uncorrected. Microanalyses were performed by the Campbell Microanalytical Laboratory, University of Otago. ^{1}H NMR spectra were measured with a Bruker Avance A400 spectrometer operating at 400.13 MHz. Chemical shifts were determined with respect to the NMR solvent. Variable temperature NMR measurements were performed with a VT BVT 3300 unit. Temperature calibration over the range 298 to 419 K was

achieved with an ethylene glycol/DMSO sample yielding the following equation $T_{actual} = -7.2663 \times 10^{-4}T_{set}^{2} + 1.5899T_{set} - 110.3$. FAB-MS spectra were recorded using a Varian VG-250S double focusing magnetic sector mass spectrometer. Samples were supported in a *p*-nitrobenzyl alcohol matrix. Electron impact (EI) mass spectra were recorded on an AEI MS 902 spectrometer at 70 eV. MALDI MS spectra were recorded using a Micromass MALDI (TOF) – Reflectron mass spectrometer operating a nitrogen UV laser at 337nm wavelength, with a dual micro-channel plate detector. Samples were supported in a *p*-nitrobenzyl alcohol matrix. Column chromatography was performed using Merck silica gel 60 Type 9835 (40–60 μm). Analytical thin layer chromatography was run on Merck silica gel 60 F_{254} pre-coated sheets (0.2 mm). Typical elutents for TLC were dichloromethane, hexane and methanol. Where solvent mixtures are used, proportions are given by volume. All solvents were AR grade which, were either used as received (methanol) or dried and distilled prior to use (dichloromethane).

Synthesis

Preparation of 3-bromo-4-methylbenzaldehyde (1). The procedure was adapted from that of Eizember and Ammons.[20] To a suspension of $AlCl_3$ (93.34 g, 0.700 mol) in refluxing dichloromethane (120 ml) under argon was added 4-methylbenzaldehyde (98%, 49.07 g, 0.400 mol) in a dropwise fashion. The reaction mixture was stirred for 30 min at 40 °C. Bromine (22.67 ml, 0.440 mol) was then added dropwise over 1 h while maintaining the reaction temperature between 30–40 °C. The resulting solution was stirred for a further 30 min, then gently poured over a stirred ice slurry (400 ml). The organic layer was diluted with $CHCl_3$ (150 ml) and separated. The aqueous layer was washed twice with $CHCl_3$ (2 × 100 ml) and the organic layers were combined and concentrated. The organic layer was washed twice with water, dried ($MgSO_4$) and reduced *in vacuo* to give a pale yellow oil that, on standing overnight, yielded colourless crystals of **1**. These were filtered, crushed and dried (70.71 g, 89%). Mp 47 °C (from $CHCl_3$; lit.[20] 48–49 °C). Found: C, 48.28; H, 3.59; Br, 40.37; C_8H_7BrO requires: C, 48.27; H, 3.54; Br, 40.14%. δ_H (400 MHz, $CDCl_3$): 2.45 (3H, s, PhCH_3), 7.37 (1H, d, *J* 7.8, Ph), 7.69 (1H, dd, *J* 7.8 and 1.1, Ph), 8.00 (1H, d, *J* 1.1, Ph), 9.88 (1H, s, CHO). EI-MS: *m*/*z* 199 (M^+, 100%).

Preparation of 1-bromo-2-methyl-5-(4,4-dimethyl-2,6-dioxan-1-yl)benzene (2). A solution of **1** (60.0 g, 0.301 mol), 2,2-dimethylpropane-1,3-diol (34.5 g, 0.331 mol) and *p*-toluenesulfonic acid (5.7 g, 30.1 mmol) in dry benzene (900 ml) was refluxed for 18 h using a Dean–Stark apparatus. Upon cooling, triethylamine (4.2 ml, 30.1 mmol) was added and the solution was reduced to dryness. The residue was purified by dissolving in CH_2Cl_2 (500 ml) and washing with water (2 × 200 ml). The organic layer was separated and dried ($MgSO_4$). The solvent was removed to give **2** as a white powder (82.05 g, 96%). Mp 59 °C (CH_2Cl_2). Found: C, 54.84; H, 5.93; Br, 27.11; $C_{13}H_{17}BrO_2$ requires: C, 54.84; H, 6.01; Br, 28.02%. δ_H (400 MHz, $CDCl_3$): 0.78 (3H, s, CH_3), 1.26 (3H, s, CH_3), 2.36 (3H, s, PhCH_3), 3.61 (2H, d, *J* 11.0, CH_2), 3.74 (2H, d, *J* 11.0, CH_2), 5.31 (1H, s, CH), 7.20 (1H, d, *J* 7.9, Ph), 7.30 (1H, dd, *J* 7.9 and 1.5, Ph), 7.67 (1H, d, *J* 1.5, Ph). EI-MS: *m*/*z* 285 (M^+, 50), 199 ($M^+ - 86$, 100%).

Preparation of 2-methyl-5-(4,4-dimethyl-2,6-dioxan-1-yl)-benzaldehyde (3). A 1.5 M solution of ^{t}BuLi in pentane (52 ml, 77.5 mmol) was slowly (over 1 h) added to a degassed solution of **2** (10.05 g, 35.2 mmol) in dry THF (200 ml) at −78 °C under argon. After 20 min at −78 °C, the solution was allowed to warm to 0 °C over 1 h, then cooled again to −78 °C. Dry DMF (6 ml, 77.5 mmol) was then added and the resulting mixture allowed to warm to 0 °C (over 50 min). An aqueous 1 M HCl solution (10 ml) was added and the resulting suspension was stirred (5 min). The aqueous layer was extracted twice with CH_2Cl_2. The combined organic layers were washed with water, dried ($MgSO_4$) and reduced *in vacuo* to give the product as a yellow oil. Purification was achieved *via* flash column chromatography (9 × 5 cm, 1 : 1 CH_2Cl_2–hexane) to give **3** as a pale yellow oil. (5.62 g, 68%). Found: C, 71.04; H, 7.48; $C_{14}H_{18}O_3$ requires C, 71.77; H, 7.74%. δ_H (400 MHz, $CDCl_3$): 0.78 (3H, s, CH_3), 1.26 (3H, s, CH_3), 2.63 (3H, s, PhCH_3), 3.64 (2H, d, *J* 11.2, CH_2), 3.75 (2H, d, *J* 11.2, CH_2), 5.40 (1H, s, CH), 7.24 (1H, d, *J* 7.8 Ph), 7.59 (1H, dd, *J* 7.8 and 1.9 Ph), 7.91 (1H, d, *J* 1.9 Ph), 10.23 (1H, s, CHO). EI-MS: *m*/*z* 234 (M^+, 45), 147 ($M^+ - 87$, 100%).

Preparation of 4. To a degassed solution of 3,3′-di-n-butyl-4,4′-dimethyl-2,2′-dipyrrolmethane (1.284 g, 4.482 mmol) and **3** (1.00 g, 4.268 mmol) in CH_2Cl_2 (430 ml) was added TFA (0.329 ml, 4.268 mmol). The resulting deep red solution was stirred for 45 min in the dark, after which time DBU (0.638 ml, 4.268 mmol) was added, followed a few minutes later by *p*-chloranil (2.623 g, 10.67 mmol). The mixture was then refluxed for 3.5 h in darkness. Upon cooling, Et_3N (2.4 ml) was added and the reaction mixture was reduced in volume (100 ml). An equal volume of MeOH was then added and the reaction was left to sit at 0 °C overnight. The intensely coloured product **4** was isolated *via* filtration as an inseparable mixture of atropisomers (1.357 g, 63.6%). δ_H (400 MHz, $CDCl_3$): −2.38 (2H, br s, NH), 0.77 (6H, s, CH_3), 1.07 (12H, t, *J* 7.3, CH_2CH_3), 1.31 (6H, s, CH_3), 1.72 (8H, m, *J* 7.3, $CH_2CH_2CH_3$), 1.96 (5.4H, s, αα-PhCH_3), 2.03 (6.6H, s, αβ-PhCH_3), 2.15 (8H, m, *J* 7.3, $CH_2CH_2CH_2$), 2.44 (12H, s, CH_3), 3.66 (4H, d, *J* 10.8, CH_2), 3.80 (4H, d, *J* 10.8, CH_2), 3.96 (8H, t, *J* 7.3, $CH_2CH_2CH_2$), 5.55 (1.1H, s, αβ-CH), 5.56 (0.9, s, αα-CH), 7.61 (0.9H, d, *J* 7.8 αα-Ph), 7.63 (1.1H, d, *J* 8.1, αα-Ph), 7.87 (2H, d, *J* 8.1, αα/αβ-Ph), 7.96 (1.1H, s, αβ-Ph), 8.04 (0.9H, s, αα-Ph), 10.19 (2H, s, meso). †

Preparation of 5. To a stirred solution of **4** (1.040 g, 1.04 mmol) in $CHCl_3$ (60 ml) was added water (20 ml) and TFA (60 ml). The biphasic mixture was left to stir under argon for 1 h. The aqueous and organic layers were diluted (an additional 100 ml in each) and the organic layer was separated. The aqueous layer was washed with $CHCl_3$ (2 × 100 ml). The organic layers were combined and washed with aqueous $NaHCO_3$ until clear (3 × 150 ml). The solution was dried ($MgSO_4$) and evaporated *in vacuo* to give **5** as a mixture of atropisomers.

Separation of the atropisomers 6-H_2 and 7-H_2. The atropisomers were separated *via* column chromatography (initial loading: 3.5 cm × 11 cm, Merck 60 silica gel, 1 : 1 CH_2Cl_2–hexane). Isomer **6**-H_2 was separated first (0–0.5% diethyl ether, 1 : 1 CH_2Cl_2–hexane) followed by isomer **7** (CH_2Cl_2, 1% diethyl ether). **6**-H_2: δ_H (400 MHz, $CDCl_3$): −2.35 (2H, br s, NH), 1.09 (12H, t, *J* 7.6, CH_2CH_3), 1.24 (12H, s, CH_3), 1.73 (8H, m, *J* 7.6, $CH_2CH_2CH_3$), 2.13 (6H, s, PhCH_3), 2.16 (8H, m, *J* 7.6, $CH_2CH_2CH_2$), 2.41 (12H, s, CH_3), 3.98 (8H, t, *J* 7.6, $CH_2CH_2CH_2$), 7.80 (2H, d, *J* 8.0, Ph), 8.25 (2H, d of d, ^1J 8.0, ^3J 1.6, Ph), 8.42 (2H, d, ^3J 1.6, Ph), 10.20 (2H, s, *meso*), 10.24 (2H, s, CHO). δ_H (400 MHz, $CD_3C_6D_5$): −1.58 (2H, br s, NH), 1.11 (12H, t, *J* 7.6, CH_2CH_3), 1.77 (8H, m, *J* 7.6, $CH_2CH_2CH_3$), 1.87 (6H, s, CH_3), 2.23 (8H, m, *J* 7.6, $CH_2CH_2CH_2$), 2.44 (12H, s, CH_3), 3.98 (8H, t, *J* 7.6, $CH_2CH_2CH_2$), 7.31 (2H, d, *J* 8.0, Ph), 8.07 (2H, d of d, ^1J 8.0, ^3J 1.2, Ph), 8.07 (2H, d, ^3J 1.2, Ph), 9.88 (2H, s, *meso*), 10.44 (2H, s, CHO). UV-vis ($CHCl_3$) λ_{max}/nm ($\varepsilon/10^3$ $dm^3\ mol^{-1}\ cm^{-1}$): 434 (445.4), 536 sh (3.6), 574 (23.0), 618 (7.7). EI-MS: *m*/*z* 827.7 (M^+, 100%). MALDI-TOF MS: *m*/*z* 827.3

† NMR assignments for the αα and αβ isomers of the free base (H_2) diacetal porphyrin were achieved by working back from the purified dialdehyde αα and αβ isomers.

(M^+, 100%). **7**-H_2: δ_H (400 MHz, $CDCl_3$): −2.29 (2H, br s, NH), 1.11 (12H, t, *J* 7.6, CH_2CH_3), 1.27 (12H, s, CH_3), 1.76 (8H, m, *J* 7.6, $CH_2CH_2CH_3$), 2.09 (6H, s, $PhCH_3$), 2.19 (8H, m, *J* 7.6, $CH_2CH_2CH_2$), 2.44 (12H, s, CH_3), 4.01 (8H, m, *J* 7.6, $CH_2CH_2CH_2$), 7.80 (2H, d, *J* 8.0, Ph), 8.27 (2H, d of d, ^1J 8.0, ^3J 1.6, Ph), 8.50 (2H, d, ^3J 1.6, Ph), 10.23 (2H, s, *meso*), 10.28 (2H, s, CHO). δ_H (400 MHz, $CD_3C_6D_5$): −1.59 (2H, br s, NH), 1.10 (12H, t, *J* 7.6, CH_2CH_3), 1.76 (8H, m, *J* 7.6, $CH_2CH_2CH_3$) 1.91 (6H, s, CH_3), 2.23 (8H, m, *J* 7.6, $CH_2CH_2CH_2$), 2.44 (12H, s, CH_3), 3.98 (8H, t, *J* 7.6, $CH_2CH_2CH_2$), 7.32 (2H, d, *J* 8.0, Ph), 8.07 (2H, d, ^1J 8.0, Ph), 8.07 (2H, s, Ph), 9.89 (2H, s, *meso*), 10.42 (2H, s, CHO). UV-vis ($CHCl_3$) λ_{max}/nm ($\varepsilon/10^3$ dm^3 mol^{-1} cm^{-1}): 434 (177.4), 538 sh (1.6), 574 (9.4), 618 (2.9). MALDI-TOF MS: *m*/*z* 827.5 (M^+, 100%).

6-Zn and 7-Zn. To **6**-H_2 or **7**-H_2 (0.030 g, 0.036 mmol) dissolved in CH_2Cl_2 (20 ml) was added $Zn(CH_3COO)_2{\cdot}2H_2O$ (0.048 g, 0.217 mmol) dissolved in MeOH (5 ml). The reaction mixture was stirred for 1 h, then reduced to dryness. The residue was dissolved in CH_2Cl_2 (10 ml) and then filtered through a silica plug to give **6**-Zn or **7**-H_2 (0.032 g, 100%). **6**-Zn (αβ isomer): δ_H (400 MHz, $CDCl_3$): 1.10 (12H, t, *J* 7.6, CH_2CH_3), 1.75 (8H, m, *J* 7.6, $CH_2CH_2CH_3$), 2.09 (6H, s, CH_3), 2.18 (8H, m, *J* 7.6, $CH_2CH_2CH_2$), 2.43 (12H, s, CH_3), 4.00 (8H, m, *J* 7.6, $CH_2CH_2CH_2$), 7.79 (2H, d, *J* 7.6, Ph), 8.27 (2H, d of d, ^1J 7.6, ^3J 1.6, Ph), 8.49 (2H, d, ^3J 1.6, Ph), 10.22 (2H, s, *meso*) 10.27 (2H, s, CHO). δ_H (400 MHz, $CD_3C_6D_5$): 1.14 (12H, t, *J* 7.6, CH_2CH_3), 1.79 (8H, m, *J* 7.6, $CH_2CH_2CH_3$), 2.01 (6H, s, CH_3), 2.26 (8H, m, *J* 7.6, $CH_2CH_2CH_2$), 2.47 (12H, s, CH_3), 4.01 (8H, t, *J* 7.6, $CH_2CH_2CH_2$), 7.38 (2H, d, *J* 8.0, Ph), 8.07 (2H, d of d, ^1J 8.0, ^3J 1.6, Ph), 8.30 (2H, d, ^3J 1.6, Ph), 9.89 (2H, s, *meso*), 10.36 (2H, s, CHO). UV-vis ($CHCl_3$) λ_{max}/nm ($\varepsilon/10^3 dm^3$ mol^{-1} cm^{-1}): 349 (20.6), 411 (288), 539 (22.5), 575 (13.9). MALDI-TOF MS: *m*/*z* 888.2 (M^+, 100%). **7**-Zn (αα isomer): δ_H (400 MHz, $CD_3C_6D_5$): 1.14 (12H, t, *J* 7.6, CH_2CH_3), 1.79 (8H, m, *J* 7.6, $CH_2CH_2CH_3$) 2.06 (6H, s, CH_3), 2.26 (8H, m, *J* 7.6, $CH_2CH_2CH_2$), 2.46 (12H, s, CH_3), 4.02 (8H, t, *J* 7.6, $CH_2CH_2CH_2$) 7.41 (2H, d, *J* 8.0, Ph), 8.11 (2H, d of d, ^1J 8.0, ^3J 1.6, Ph), 8.24 (2H, d, ^3J 1.6, Ph), 9.88 (2H, s, *meso*), 10.35 (2H, s, CHO). MALDI-TOF MS: *m*/*z* 888.2 (M^+, 100%).

6-Ni and 7-Ni. To $Ni(CH_3COO)_2{\cdot}4H_2O$ (0.331 g, 0.133 mmol) suspended in MeOH was added **6** or **7** (0.137 g, 0.166 mmol) dissolved in $CHCl_3$ (50 ml). The resulting mixture was refluxed for 2 days under an inert atmosphere in darkness. After cooling, the solvent was removed and the resulting residue was dissolved in CH_2Cl_2 (20 ml) and filtered through a silica plug to give **6**-Ni or **7**-Ni (0.138 g, 95%). No sign of atropisomerism was observed during the metallation process. **6**-Ni (αβ isomer): δ_H (400 MHz, $CDCl_3$): 1.07 (12H, t, *J* 7.4, CH_2CH_3), 1.65 (8H, m, *J* 7.4, $CH_2CH_2CH_3$), 2.02 (8H, m, *J* 7.4, $CH_2CH_2CH_2$), 2.09 (6H, s, CH_3), 2.18 (12H, s, CH_3), 3.68 (8H, m, *J* 7.4, $CH_2CH_2CH_2$) 7.69 (2H, d, *J* 8.0, Ph), 8.16 (2H, d of d, ^1J 8.0, ^3J 1.6, Ph) 8.25 (2H, d, ^3J 1.6, Ph), 9.47 (2H, s, *meso*) 10.14 (2H, s, CHO). δ_H (400 MHz, $CD_3C_6D_5$): 1.03 (12H, t, *J* 7.6, CH_2CH_3), 1.63 (8H, m, *J* 7.6, $CH_2CH_2CH_3$) 1.84 (6H, s, CH_3), 2.05 (8H, m, *J* 7.6, $CH_2CH_2CH_2$), 2.18 (12H, s, CH_3), 3.66 (8H, t, *J* 7.6, $CH_2CH_2CH_2$), 7.29 (2H, d, *J* 8.0, Ph), 7.93 (2H, d of d, ^1J 8.0, ^3J 1.6, Ph), 8.04 (2H, d, ^3J 1.6, Ph), 9.61 (2H, s, CHO), 9.91 (2H, s, *meso*). UV-vis ($CHCl_3$) λ_{max}/nm ($\varepsilon/10^3$ dm^3 mol^{-1} cm^{-1}): 350 (13.7), 410 (275.3), 531 (19.5), 566 (26.5). MALDI-TOF MS: *m*/*z* 882.2 (M^+, 100%). **7**-Ni (αα isomer): δ_H (400 MHz, $CDCl_3$): 1.05 (12H, t, *J* 7.2, CH_2CH_3), 1.63 (8H, m, *J* 7.2, $CH_2CH_2CH_3$), 2.00 (6H, s, CH_3), 2.00 (8H, m, *J* 7.2, $CH_2CH_2CH_2$), 2.16 (12H, s, CH_3), 3.66 (8H, t, *J* 7.2, $CH_2CH_2CH_2$), 7.66 (2H, d, *J* 7.6, Ph), 8.15 (2H, d, *J* 7.6, Ph), 8.31 (2H, s, Ph), 9.45 (2H, s, CHO), 10.14 (2H, s, *meso*). δ_H (400 MHz, $CD_3C_6D_5$): 1.03 (12H, t, *J* 7.6, CH_2CH_3), 1.63 (8H, m, *J* 7.6, $CH_2CH_2CH_3$), 1.84 (6H, s, CH_3), 2.05 (8H, m, *J* 7.6, $CH_2CH_2CH_2$), 2.18 (12H, s, CH_3), 3.66 (8H, t, *J* 7.6, $CH_2CH_2CH_2$), 7.29 (2H, d, *J* 8.0, Ph), 7.94 (2H, d of d, ^1J 8.0, ^3J 1.6, Ph), 8.03 (2H, d, ^3J 1.6, Ph), 9.62 (2H, s, CHO), 9.90 (2H, s, *meso*). UV-vis ($CHCl_3$) λ_{max}/nm ($\varepsilon/10^3$ dm^3 mol^{-1} cm^{-1}): 324 (18.4), 410 (186.5), 531 (11.4), 566 (16.8). MALDI-TOF MS: *m*/*z* 882.3 (M^+, 100%).

6-Cu and 7-Cu. Procedure as for nickel. **6**-Cu (αβ isomer): UV-vis ($CHCl_3$) λ_{max}/nm ($\varepsilon/10^3$ dm^3 mol^{-1} cm^{-1}): 334 (22.1), 411 (304.5), 534 (15.1), 570 (14.0). MALDI-TOF MS: *m*/*z* 888.3 (M^+, 100%). **7**-Cu (αα isomer): UV-vis ($CHCl_3$) λ_{max}/nm ($\varepsilon/10^3$ dm^3 mol^{-1} cm^{-1}): 332 (4.9), 411 (277.1), 534 (12.6), 570 (11.9). MALDI-TOF MS: *m*/*z* 888.3 (M^+, 100%).

Kinetic studies

The porphyrin to be studied was dissolved into d^8 toluene (typical concentration 5 mmol l^{-1}) and placed into a pressure NMR tube which was then sealed. The sample was heated at a fixed temperature for a set period of time. Accurate proton integrations could not be determined from the ^1H spectrum of the atropisomers at elevated temperatures due to the overlap of signals of interest; therefore, the reaction was quenched by cooling the sample rapidly to room temperature and the ^1H NMR spectrum was recorded. Rates were determined from a plot of change in concentration of reactant against time, which follows first-order kinetics in the initial stages of the interconversion. Rates were determined from extrapolation of several data points. Typically, 10–15 data points were used for the majority of temperatures (at the very highest temperature, the rate of reaction was such that only 3 points could be obtained). Enthalpy values were determined from an Arrenhius plot over five different temperatures (three for **7**-Ni).

Acknowledgements

The authors would like to thank Pat Edwards for the temperature calibration data and the Marsden fund for support for P. G. P.

References

1 J. P. Collman, R. R. Gagne, C. Reed, T. R. Halbert, G. Lang and W. T. Robinson, *J. Am. Chem. Soc.*, 1975, **97**, 1427; J. P. Collman, R. R. Gagne, T. R. Halbert, J. C. Marchon and C. A. Reed, *J. Am. Chem. Soc.*, 1973, **95**, 7868; J. P. Collman and T. N. Sorrell, *J. Am. Chem. Soc.*, 1975, **97**, 4133; J. P. Collman, T. N. Sorrell and B. M. Hoffman, *J. Am. Chem. Soc.*, 1975, **97**, 913.
2 Y. Kuroda, Y. Kato, M. Ito, J.-Y. Hasegawa and H. Ogoshi, *J. Am. Chem. Soc.*, 1994, **116**, 10338; P. Le Maux, H. Bahri and G. Simonneaux, *J. Chem. Soc., Chem. Commun.*, 1991, 1350; E. Galardon, P. L. Maux, L. Toupet and G. Simonneaux, *Organometallics*, 1998, **17**, 565.
3 T. Arai, A. Tsukuni, K. Kawazu, H. Aoi, T. Hamada and N. Nishino, *J. Chem. Soc., Perkin Trans. 2*, 2000, 1381.
4 S. B. Ungashe and J. T. Groves, *Adv. Inorg. Biochem.*, 1994, **9**, 317; J. Lahiri, G. D. Fate, S. B. Ungashe and J. T. Groves, *J. Am. Chem. Soc.*, 1996, **118**, 2347.
5 J. K. M. Sanders, *Compr. Supramol. Chem.*, 1996, **9**, 131.
6 L. K. Gottwald and E. F. Ullman, *Tetrahedron Lett.*, 1969, 3071.
7 R. A. Freitag and D. G. Whitten, *J. Phys. Chem.*, 1983, **87**, 3918.
8 J. W. Dirks, G. Underwood, J. C. Matheson and D. Gust, *J. Org. Chem.*, 1979, **44**, 2551.
9 F. A. Walker, *Tetrahedron Lett.*, 1971, 4949; M. J. Crossley, L. D. Field, A. J. Forster, M. M. Harding and S. Sternhell, *J. Am. Chem. Soc.*, 1987, **109**, 341; K. Hatano, K. Anzai, T. Kubo and S. Tamai, *Bull. Chem. Soc. Jpn.*, 1981, **54**, 3518; K. Hatano, K. Anzai, A. Nishino and K. Fujii, *Bull. Chem. Soc. Jpn.*, 1985, **58**, 3653; T. Fujimoto, H. Umekawa and N. Nishino, *Chem. Lett.*, 1992, 37; I. Spasojevic, R. Onzeleev, P. S. White and I. Fridovich, *Inorg. Chem.*, 2002, **41**, 5874; R. Song, A. Robert, J. Bernadou and B. Meunier, *Analusis*, 1999, **27**, 464; G. Reginato, L. Di Bari, P. Salvadori and R. Guilard, *Eur. J. Org. Chem.*, 2000, 1165.
10 K. Hatano, K. Kawasaki, S. Munakata and Y. Iitaka, *Bull. Chem. Soc. Jpn.*, 1987, **60**, 1985.
11 B. Zimmer, V. Bulach, C. Drexler, S. Erhardt, M. W. Hosseini and A. De Cian, *New J. Chem.*, 2002, **26**, 43.

12 X.-X. Zhang and S. J. Lippard, *J. Org. Chem.*, 2000, **65**, 5298; C. Comte, C. P. Gros, R. Guilard, R. G. Khoury and K. M. Smith, *J. Porphyrins Phthalocyanines*, 1998, **2**, 377.
13 J. E. Redman and J. K. M. Sanders, *Org. Lett.*, 2000, **2**, 4141.
14 G. M. Sanders, M. Van Dijk, B. M. Machiels and A. Van Veldhuizen, *J. Org. Chem.*, 1991, **56**, 1301; M. J. Gunter and L. N. Mander, *J. Org. Chem.*, 1981, **46**, 4792; X. Shi, S. R. Amin and L. S. Liebeskind, *J. Org. Chem.*, 2000, **65**, 1650; Y. Aoyama, T. Kamohara, A. Yamagishi, H. Toi and H. Ogoshi, *Tetrahedron Lett.*, 1987, **28**, 2143; H. Ogoshi and T. Mizutani, *Acc. Chem. Res.*, 1998, **31**, 81.
15 R. Young and C. K. Chang, *J. Am. Chem. Soc.*, 1985, **107**, 898.
16 K. Konishi, K. Miyazaki, T. Aida and S. Inoue, *J. Am. Chem. Soc.*, 1990, **112**, 5639.
17 J.-F. Nierengarten and J.-F. Nicoud, *Chem. Commun.*, 1998, 1545; W. J. Belcher, A. K. Burrell, W. M. Campbell, D. L. Officer, D. C. W. Reid and K. Y. Wild, *Tetrahedron*, 1999, **55**, 2401.
18 Y. Okuno, T. Kamikado, S. Yokoyama and S. Mashiko, *THEOCHEM*, 2002, **594**, 55.
19 J. L. Sessler, M. R. Johnson, S. E. Creager, J. C. Fettinger and J. A. Ibers, *J. Am. Chem. Soc.*, 1990, **112**, 9310.
20 R. F. Eizember and A. S. Ammons, *Org. Prep. Proced. Int.*, 1974, **6**, 251.
21 P. Van der Sluis and A. L. Spek, *Acta Crystallogr., Sect. A*, 1990, **46**, 194.
22 K. J. Laidler and J. H. Meiser, in *Physical Chemistry*, ed. G. Hubit, Benjamin/Cummings, New York, 1982, ch. 9.
23 S. S. Eaton and G. R. Eaton, *J. Am. Chem. Soc.*, 1977, **99**, 6594.